RSC Advances

ROYAL SOCIETY OF CHEMISTRY

www.rsc.org/advances

Journal Name

ARTICLE

Hydrothermal synthesis of Co-ZnO nanowire array and its application as piezo-driven self-powered humidity sensor with high sensitivity and repeatability

Received 00th January 20xx,
Accepted 00th January 20xx

DOI: 10.1039/x0xx00000x

www.rsc.org/

Weili Zang, Pan Li, Yongming Fu, Lili Xing* and Xinyu Xue*

High sensitive and repeatable self-powered humidity sensor has been realized from Co-doped ZnO nanowires (NWs). The piezoelectric output of the device acts not only as a power source, but also as a response signal to the relative humidity (RH) in the environment. When the relative humidity is 70% RH at room temperature, the piezoelectric output voltage of the humidity sensor under compressive force decreases from 1.004 (at 20% RH) to 0.181 V. The sensitivity of self-powered humidity sensing based on Co-doped ZnO nanoarrays is much higher than that of undoped ZnO nanoarrays. The device exhibits good repeatability for humidity detection, and the response maintains ~90% after one month. Such a high performance can be attributed to the piezo-surface coupling effect of the nanocomposites and more active sites introduced by the Co dopants. Our study can stimulate a research trend on exploring composite materials for piezo-gas sensing.

Introduction

Humidity sensors are important devices that have been extensively used in our daily life.[1-3] These devices can monitor the environmental moisture for human comfort. Humidity sensors can also be used in automotive, medical, construction, meteorological and food processing industries. Traditional humidity sensors operate by testing the change of electrical resistance or capacitance upon exposure to a humid environment. In this case, external electronic power source or batteries are needed to power these electronic sensors, which is not environment-friendly and portable.[4-7] Recently, much research effort has been made on developing new technologies in the fields of green energy harvesting and gas sensing.[8-12] Most recently, a new self-powered system that integrates energy generator and functional nanodevice has been proposed, aiming at harvesting energy from the environment to power the functional nanodevice with no need for external electronic, such as self-powered pH sensors, self-powered pressure/speed sensor and self-powered AC magnetic sensor.[13-16] In our previous reports, a self-powered/active humidity sensor based on ZnO nanowires (NWs) nanogenerator (NG) has been firstly demonstrated by coupling the piezoelectric and humidity sensing characteristics of ZnO NW, in which the piezoelectric output of the device can be influenced by test gas ambience.[17] Thus the piezoelectric can act not only as a power source, but also as a response signal to the relative humidity (RH). However, the sensing performance of ZnO based self-powered humidity sensor is relatively low (low sensitivity and poor reliability), which restrains their practical applications. For traditional resistance-type gas sensing materials, doping with transition metal ions in oxide semiconductor is a very effective way to improve their sensing properties. For example, Co-doped ZnO based sensors exhibit improved gas sensing performance compared to pure ZnO sensors, thanks to the impurity energy levels[18,19] and more active sites introduced by the Co dopants[20]. Thus it is expected that the performance of self-powered gas sensor can be enhanced by introducing Co dopant into the ZnO NW.

In this paper, self-powered humidity sensor with high sensitivity and repeatability has been fabricated from Co-doped ZnO NW arrays. By doping Co in ZnO, donor-related oxygen vacancies are introduced, which provides more adsorption sites for water molecules, resulting in a high sensitivity against the RH.

Experimental

The vertically-aligned Co-doped ZnO NW arrays were synthesized by a seed-assisted wet-chemical method. Firstly, Zinc acetate dehydrate was dissolved in ethanol with a concentration of 10 mM. A droplet of solution was coated onto pre-cleaned Ti substrate, and then blown dry with nitrogen gas. The coated substrate was annealed at 350°C for 20 min in air to yield a layer of ZnO seeds, as shown in Fig. 1a. After that, Co-doped ZnO NW arrays were synthesized via a

College of Sciences, Northeastern University, Shenyang, 110004, China. E-mail: xingrenyier@sina.com; xuexinyu@mail.neu.edu.cn.

† Footnotes relating to the title and/or authors should appear here.
Electronic Supplementary Information (ESI) available: [details of any supplementary information available should be included here]. See DOI: 10.1039/x0xx00000x

hydrothermal route in 50 mL of aqueous solution of $Zn(NO_3)_2{\cdot}6H_2O$ (25 mM), $C_6H_{12}N_4$ (HMTA, 25 mM) and $Co(CH_3COO)_2{\cdot}4H_2O$ (10 mM) in a reaction flask at 80°C. In the growth process, Zn^{2+} and Co^{2+} are provided by hydration of

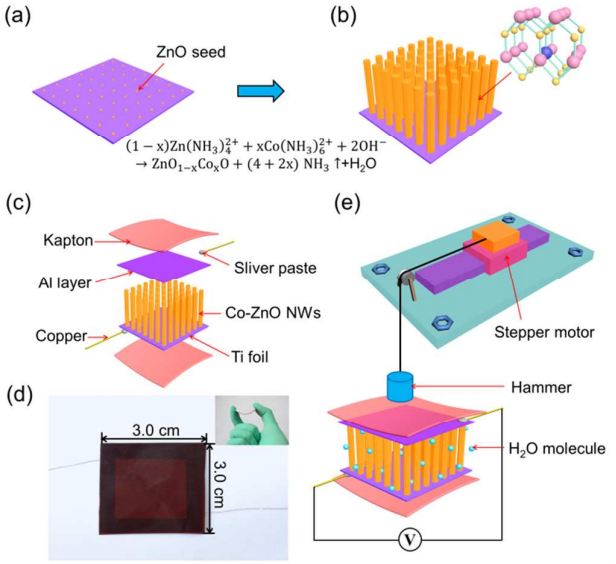

Fig. 1 Fabrication process of the self-powered humidity sensor based on Co-doped ZnO NW arrays. (a) ZnO seeds are deposited on the pre-cleaned Ti foil. (b) Co-doped ZnO NWs are vertically aligned on the substrate via a hydrothermal route. (c) Schematic diagram showing the structural design of self-powered humidity sensor. (d) Optical image of a device, demonstrating the flexibility. (e) Schematic image showing the device actively detecting humidity.

$Zn(NO_3)_2$ and $Co(CH_3COO)_2$. HMTA acts as a pH buffer to regulate pH value of the solution and the slow supply of OH^- and NH_4^+.[21] This can be explained by simple chemical reaction:

$$(CH_2)_6N_4 + 6H_2O \rightarrow 4NH_3 + 6HCHO$$
$$NH_3 + H_2O \rightarrow NH_4^+ + OH^-$$

In this high NH_3 concentration environment, most of the zinc Zn^{2+} ions form the amine complex $Zn(NH_3)_4^{2+}$. Co^{2+} ions in solution remained octahedrally coordinated until the nucleation of ZnO crystallites, where they bind to the nanocrystal surfaces with tetrahedral geometries as monomers.[22] The following formulas can be used to illustrate the Co-doped ZnO NW growth mechanism:

$$Zn^{2+} + 4NH_3 \leftrightarrow Zn(NH_3)_4^{2+}$$
$$Co^{2+} + 4NH_3 \leftrightarrow Co(NH_3)_4^{2+}$$
$$(1-x)Zn(NH_3)_4^{2+} + xCo(NH_3)_4^{2+} + 2OH^- \rightarrow Zn_{1-x}Co_xO + (4+2x)NH_3 \uparrow + H_2O$$

After reaction for 12 h, the Ti substrate coated with vertically-aligned Co-doped ZnO NW arrays was removed from the solution, rinsed with deionized water and ethanol, and dried at 60°C.

The structure of the self-powered humidity sensor is shown in Fig. 1c. The device is composed of three major components: Co-doped ZnO NW arrays on Ti foil, Al layer and Kapton films. Such a device structure is similar to a typical NG without packaging. Ti foil acts as both the substrate for Co-doped ZnO NW arrays and the conductive electrode. A piece of Al foil (thickness=0.05 mm) positioned on the top of Co-doped

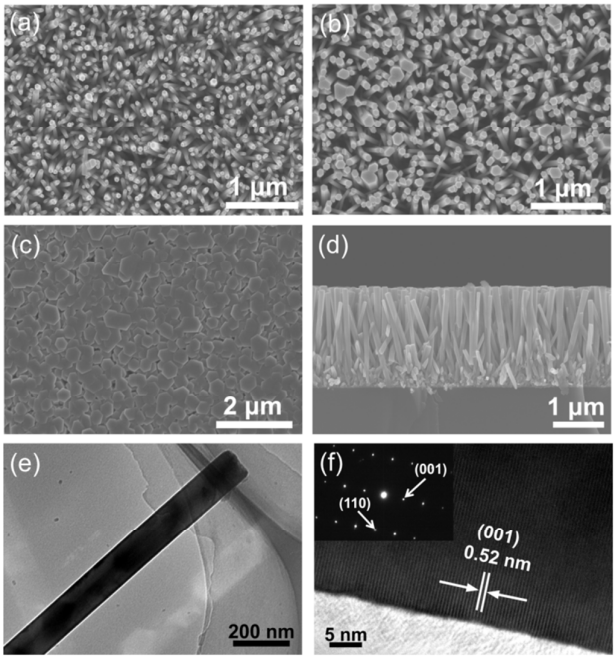

Fig. 2 (a-c) Top view SEM images of Co-doped ZnO NW arrays with the 5 mM, 10 mM and 15mM of dopant in reactive solution. (d) SEM image of Co-doped ZnO NW arrays in a side view. (e) TEM image of one single Co-doped ZnO NW. (f) HRTEM and SAED pattern of the tip region of Co-doped ZnO NW.

ZnO NW arrays acts as counter electrode. The device was tightly fixed between two sheets of flexible Kapton film (3.0×3.0 cm in area) as the support frames to ensure the electric contacts between the electrodes and the NWs. In fact, the height of the NWs is quasi-uniform, and the NWs are not perfectly vertically aligned, which leads to few effective contacts between NWs and electrodes. But the 50-μm-thick Kapton film as the flexible substrates are soft and can be sufficiently bent to follow the height profiles of NWs, which can enhance the effective contacts.[23] Fig. 1d displays the photograph of the self-powered humidity sensor, and the inset indicates that the device is flexible and can be easily bent by human hand.The schematic diagram of test system is showed in Fig. 1e. The sensing performance of the self-powered humidity sensor was studied by measuring the piezoelectric output against different RH under constant applied compressive strain. A compressive force was applied to the device by a hammer actuated by a stepper motor moved along a guide rail (the movement of the motor can be controlled by programming). The compressive force applied on the device was 34 N at the frequency of 1 Hz. Under externally applied compressive deformation, the piezoelectric output of the device can act as both the power source and the humidity sensing signal. The sensor was connected to a low-noise preamplifier (Model SR560, Stanford Research Systems) for measuring the piezoelectric output voltage. In order to improve the signal to noise ratio, the device was aged under the applying force (34 N, 1 Hz) for 72 h at room temperature. This aging process could stabilize the piezoelectric output. And

in this process, the surface adsorption of water molecules could reach equilibrium.

Results and discussion

The morphology of Co-doped ZnO NW arrays was characterized by scanning electron microscopy (SEM, Hitachi S4800). Fig. 2a-c show the top-view SEM images of Co-doped ZnO NW arrays with different concentration of the dopant in reactive solution. It should be noted that the morphology and diameter is dependent on the doping concentration of Co. As the concentration of the dopant in reactive solution is tuned to 5, 10, 15 mM, the corresponding diameter is 80, 130, 350 nm, respectively. Due to the smaller radius of Zn^{2+} (0.74 Å) compared with that of Co^{2+} (0.82 Å),[24] the replacement of Zn^{2+} by Co^{2+} in crystal structure leads to slight increases in diameter, suggesting that more Co^{2+} is doped into ZnO NWs. Fig. 2d is a side-view SEM image of Co-doped ZnO NW arrays with 10 mM of dopant in reactive solution. It can be seen that hexagonal Co-doped ZnO NW arrays are densely grown on Ti substrate along a consistent growth direction. And it reveals that the average length of the NWs is about 2.1 μm. Fig. 2e is a transmission electron microscopy (TEM) image of one single Co-doped ZnO NW, showing that the whole surface of the NW is very smooth. In order to further determine the structure and composition of Co-doped ZnO NWs, high-resolution TEM (HRTEM) and select area electron diffraction (SAED) were performed, as shown in Fig. 2f. The lattice spacing of 0.52 nm, consistent with (001) crystal plane of wurtzite structural ZnO, indicates that the NW grows along [0001] direction. The SAED pattern of the NW clearly shows single-crystalline nature of ZnO structure.

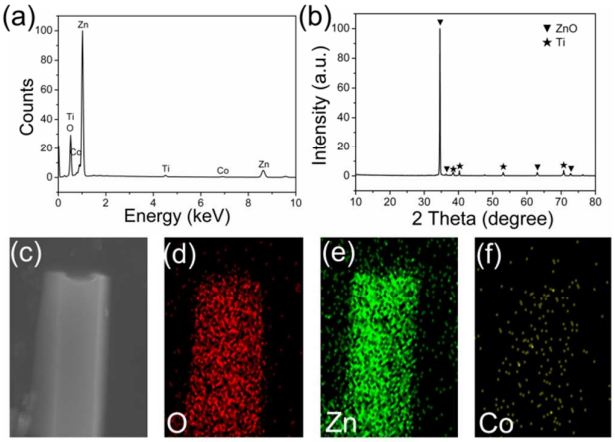

Fig. 3 (a) and (b) XRD pattern and EDS spectrum of Co-doped ZnO NWs, respectively. (c-f) Elemental mapping crossing one single Co-doped ZnO NW.

The composition of Co-doped ZnO (10 mM) nanoarrays was determined by energy dispersive spectrometer (EDS) (Fig. 3a), and the result shows the existence of Co, Zn, O and Ti in the spectrum, in which Ti elements come from the Ti foil substrate. By analyzing the EDS results, the atomic percentage of Co element is about 0.72%. Similar EDS results have been obtained at other different areas, which indicates that Co has uniformly doped into ZnO NWs. The crystal phase of Co-doped ZnO NW arrays was characterized by X-ray powder diffraction (XRD; D/max 2500 V, Cu K_α radiation, λ=1.5405 Å). The XRD pattern of Co-doped ZnO NW arrays on Ti substrate is shown in Fig. 3b, and the sharp diffraction peaks indicate the good crystalline quality. The peaks marked by pentagram can be indexed to Ti (JCPDS file No. 44-1294) arising from the Ti foil substrate; the peaks marked by inverted triangle are in good agreement with the hexagonal wurtzite ZnO (JCPDS file No. 36-1451). No other phase can be observed, which indicates that the Co^{2+} ions have substituted Zn^{2+} ions in the samples without changing its crystal structure. Fig. 3c-f show the elemental mapping crossing one single Co-doped ZnO NW, which indicates that O, Zn and Co are uniformly distributed in the sample. These results confirm that Co element is uniformly doped into ZnO NWs.

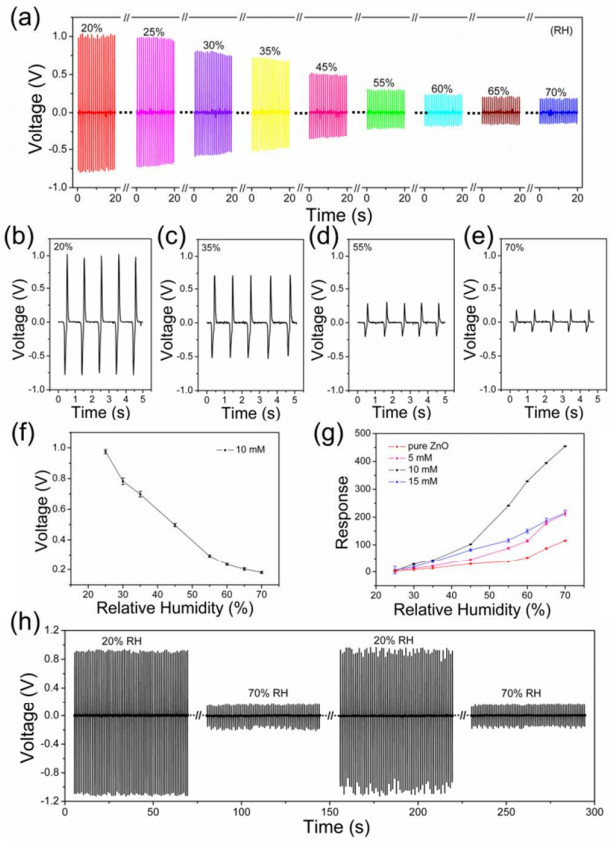

Fig. 4 (a) The piezoelectric output voltage of the device at different humidity conditions under the same applied strain at room temperature. (b–e) The enlarged images of the output voltage at 20%, 35%, 55% and 70% RH, respectively. (f) The relationship between the piezoelectric output voltage and relative humidity. (g) The response of Co-doped ZnO NWs with different concentration of cobalt in reactive solution. (h) The recovery and repeatability of the self-powered active humidity sensor.

Fig. 4a is the piezoelectric output voltage of Co-doped ZnO (10 mM) NW arrays against different relative humidity conditions ranging from 20% to 70% under the same applied force (34 N, 1 Hz) at room temperature. When the relative

humidity is 20%, 25%, 30%, 35%, 45%, 55%, 60%, 65% and 70%, the piezoelectric output voltage of the device is 1.004, 0.975, 0.782, 0.698, 0.496, 0.294, 0.234, 0.203 and 0.181 V, respectively. Fig. 4b-e are the enlarged views of the piezoelectric output of the device at 20%, 35%, 55% and 70% RH. The relationship between the piezoelectric output voltage and relative humidity was shown in Fig. 4f. It can be seen that the piezoelectric voltage significantly decreases as the relative humidity increases. Similar to the traditional definition of the sensitivity of resistance-type gas sensors ($S\% = \frac{R_a - R_g}{R_g} \times 100\%$,[25] where R_a and R_g represent the resistance of the sensor in dry air and in the test gas, respectively), the response R of the self-powered humidity sensor under the same deformation conditions can be simply defined as:

$$R\% = \frac{|V_0 - V_t|}{V_t} \times 100\%$$

in which V_0 represents the piezoelectric output voltage of Co-doped ZnO NWs against 20% RH, and V_t represents the output voltage at the test relative humidity. As shown in Fig. 4g, the response of Co-doped ZnO NW arrays against 25%, 30%, 35%, 45%, 55%, 60%, 65% and 70% RH at room temperature is 3, 28.3, 43.9, 102.3, 241.2, 328.7, 394.3 and 454.2, respectively. Against 70% RH, as the concentration of the dopant in reactive solution is tuned to 0, 5, 10, 15 mM, the corresponding response is 120.6, 200.7, 454.2, 226.9, respectively. It can be seen that the response of Co-doped ZnO NWs is related to both the doping concentration and NW dimensions, and 10 mM Co-doped ZnO has higher sensitivity than that of 0, 5 and 15 mM Co-doped ZnO NWs. When the concentration of the dopant in reactive solution is lower than 10 mM, the response increases with increasing Co doping concentration duo to that Co dopant can introduce oxygen vacancies for water adsorption. On the other hand, when the concentration of the dopant in reactive solution is 15 mM, the excessive Co dopant in NWs significantly decreases the specific surface area and thus decreases the humidity-sensing performance. Co-doped ZnO NW arrays with 10 mM of cobalt in reactive solution have potential applications in self-powered humidity sensors.

The responding–recovering process of the self-powered active humidity sensor against 70% RH is shown in Fig.4h. When the relative humidity increases from 20% to 70%, the piezoelectric output voltage decreases from 0.91 to 0.16 V. After the atmosphere of the test chamber is rapidly changed to 20% RH, the piezo-voltage of the device recovers to the original value. And the humidity response against 70% RH can be repeated. Also, the humidity sensing performance has been investigated for more than 20 devices, and the response behavior of the devices is similar. This result demonstrates good recovery and repeatability of the device.

Table 1 shows the comparison between Co-doped ZnO NW humidity sensor and other previous results. It can be seen that Co-doped ZnO nanowire NG as a self-powered active humidity sensor can convert mechanical energy into electric power as response signal of relative humidity. And the self-powered humidity sensing performance of Co-doped ZnO NWs is higher than that of other self-powered humidity sensors.

Table 1. Comparison of humidity sensing performance.

Materials	Type	RH (%)	R	Ref.
ZnO nanoparticles	Resistance	78	122	26
ZnO nanorods	Capacitance	97	225	27
TiO_2-ZnO nanorods	Resistance	70	775	28
CeO_2/ZnO NWs	Piezoelectric	85	350	29
Sb-ZnO NWs	Piezoelectric	70	390	30
Fe-ZnO NWs	Piezoelectric	60	305	31
ZnO NWs	Piezoelectric	70	115	This work
Co-ZnO NWs	Piezoelectric	70	457	This work

Stability is one of the most important aspects of gas sensing system, especially for its practical applications. Fig. 5 exhibits the repeatability of Co-doped ZnO NW humidity sensor. Fig. 5a and b are top and side view SEM image of Co-doped ZnO NW arrays after ~50000-time deformations, respectively. Fig. 5c shows the piezoelectric output voltage of the device against various humidity conditions after one month. When the relative humidity is 20%, 25%, 30%, 35%, 45%, 55%, 60%, 65% and 70%, the piezoelectric output voltage of the device is 0.909, 0.906, 0.788, 0.632, 0.454, 0.273, 0.232, 0.192 and 0.177 V, respectively. As shown in Fig. 5d, after 50000-time deformations, the response of the device against 25%, 30%, 35%, 45%, 55%, 60%, 65% and 70% RH is 4.1, 28.3, 44.5, 106.5, 248.9, 324.0, 382.4 and 419.6, respectively. After one month, the response of the device against 25%, 30%, 35%, 45%, 55%, 60%, 65% and 70% RH is 0.2, 15.3, 43.7, 100.1, 232.8, 291.8, 373.2, and 413.6, respectively. The response maintains ~90% compared with the original results, indicating a relatively high repeatability for humidity detection.

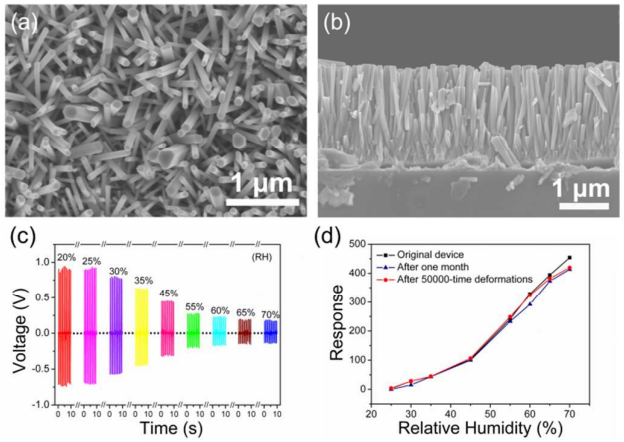

Fig. 5 (a, b) SEM images of Co-doped ZnO NWs after 50000-time deformations on the top and side view, respectively. (c) The piezoelectric output voltage of the device against different relative humidity after one month. (d) The response decline after 50000-time deformations and after one month.

The high piezo-humidity sensing can be ascribed to the new piezo-surface coupling effect of the nanocomposites.[32] The piezoelectric effect is understood as when piezoelectric material is applied under mechanical stress and deformed, internal polarization takes place, leading to the appearance of positive charge on one surface and negative charge on the opposite surface. The piezoelectric field can drive electrons in

the outside circuit to flow (piezoelectric output). At the same time, the free electrons in ZnO NWs will transfer and partially screen this piezoelectric field and decrease the piezoelectric output (piezoelectric screening effect).[33] The surface effect is a mechanism that the specific surface area and the number of surface atoms significantly increase with decreasing diameter of material, leading to the high chemical/physical activity (such as highly-sensitive gas sensing).[34] Previous theoretical and experimental works have confirmed that the electron concentration of ZnO NW arrays can be affected by the gas adsorption on the surface, which greatly changes the piezoelectric screening effect and thus affects the piezoelectric output of the device.[29, 35, 36] The doping with transition metal ions in oxide semiconductor is one of the routes to improve their sensing properties. Some former researches have proved that the existence of cobalt species in semiconductor sensing materials can improve their sensitivity prominently.[18,37,38] In this paper, Co doping induces abundant donor-related oxygen vacancies, which provide more adsorption sites for oxygen molecules.[39, 40] The high surface adsorption of oxygen is the key for obtaining an excellent gas-sensing performance of the sensor. When the device is in a humid environment, more water molecules can displace these oxygen vacancies, resulting in an increase of free electrons. The free carriers are significantly increased, and the piezoelectric screening effect is enhanced, resulting in a high sensitivity against the relative humidity.

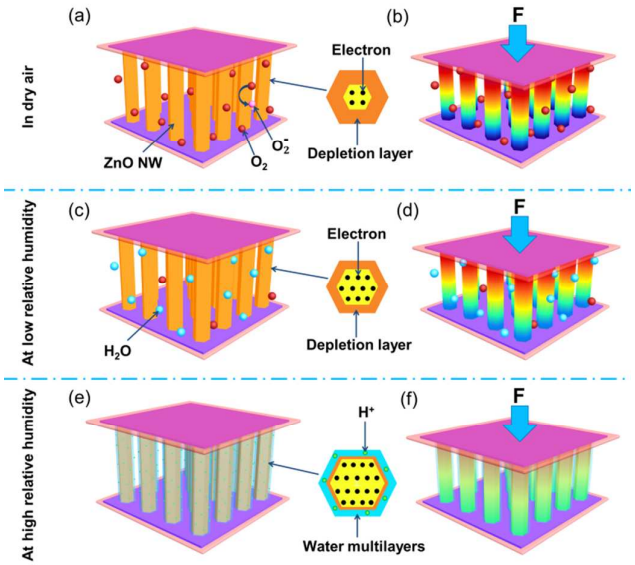

Fig. 6 The working mechanism of the self-powered humidity sensor based on Co-doped ZnO NW arrays. (a) Schematic illustration of the depletion layer in NWs in dry air without compressive force. (b) Schematic illustration of the piezoelectric output of the device in dry air under compressive force. (c) Schematic illustration showing Co-doped ZnO NW arrays at low relative humidity without applied force. (d) The piezoelectric output of the device under mechanical deformation at low relative humidity. (e) Co-doped ZnO NW without compression at high relative humidity. (f) The piezoelectric output of the device under mechanical deformation at high relative humidity.

The detailed working mechanism of the self-powered humidity sensor based on Co-doped ZnO NW arrays is shown in Fig. 6. By doping Co in ZnO, impurity energy levels are introduced. Therefore, the Fermi level of Co-doped ZnO moves closer toward conduction band than that without doping and produces a large amount of free electrons.[19] According to our previous theoretical works, the output piezo-voltage (V_{out}) of gas sensor can be given by:[32]

$$V_{out} = \frac{\gamma e_{33} \cdot s_{33} \cdot d}{\varepsilon_s \cdot N_D}$$

in which s_{33} is the strain of the material, d is the distance between the two current collectors, ε_s is the permittivity of the material, e_{33} is piezoelectric constant, N_D is the donor concentration inherent in the material, and γ is a factor dependent on the material system and the device structure.

The oxygen vacancies mainly spread near the surface, resulting in many adsorption sites on the surface of the NWs. A large amount of oxygen molecules can be adsorbed on the surface of Co-doped ZnO NWs and form O_2^- ions by capturing free electrons from the NWs.[41,42] This leads to a thick depletion layer on the surface of NWs, and therefore result in a decrease of free electrons. When the device is under a compressive strain (Fig. 6b), a piezoelectric field is created along NWs. The free electron density of Co-doped ZnO NWs is low; thus, the screening effect is weak and the piezoelectric output is high. The output piezo-voltage (V_{out}) of gas sensor can be simply described as follows:

$$V_{out} = \frac{\gamma e_{33} \cdot s_{33} \cdot d}{\varepsilon_s \cdot (N_D - N_{O_2^-})}$$

in which $N_{O_2^-}$ is the concentration of oxygen molecules adsorbed on the surface of NWs.

When the device is at low relative humidity without any applied force (Fig. 6c), water molecules quickly displace the oxygen ions and release free electrons back into the NWs, resulting in a decrease in the depletion layer. With increasing relative humidity, more oxygen ions are displaced by water molecules, resulting in more free electrons inside of the Co-doped ZnO NWs and a thinner surface depletion layer. At the same time, in addition to the chemisorbed water forms, the physisorbed water dissociates into H_3O^+ and OH^- ions because of the high electrostatic field in the chemisorbed layer. H_3O^+ appears in the physisorbed water and serves as a charge carrier by a Grotthuss chain reaction in H_2O-Co-ZnO NWs.[43,44] When a compressive force is applied on the device, the output piezo-voltage (V_{out}) of gas sensor can be simply described as follows:

$$V_{out} = \frac{\gamma e_{33} \cdot s_{33} \cdot d}{\varepsilon_s \cdot (N_D + N_{H_3O^+})}$$

in which $N_{H_3O^+}$ is the concentration of vapour molecules adsorbed on the surface of NWs. Both the conductive H_3O^+ outside the NWs and the increased free electrons inside the Co-doped ZnO NWs can screen the piezoelectric polarization charges in the NWs, thus the piezoelectric output voltage of the humidity sensor is lowered, as shown in Fig. 6d.

At high relative humidity (Fig. 6e), The majority of adsorption sites are occupied by continuous water molecule, which leads to a thinner depletion layer on the surface of NWs and physisorbed water multilayers. The protons will gain

freedom to move randomly inside the water multilayers.[45] The output piezo-voltage (V_{out}) of gas sensor can be simply described as follows:

$$V_{out} = \frac{\gamma e_{33} \cdot s_{33} \cdot d}{\varepsilon_s \cdot (N_D + N_{H_3O^+} + N_{H^+})}$$

in which N_{H^+} is the concentration of protons in the water multilayers. When a compressive strain is applied on the device at high relative humidity (Fig. 6f), the protons in the water layer and high density electrons inside the NWs will lead to an enhanced screen effect and result in a very low piezoelectric output voltage.

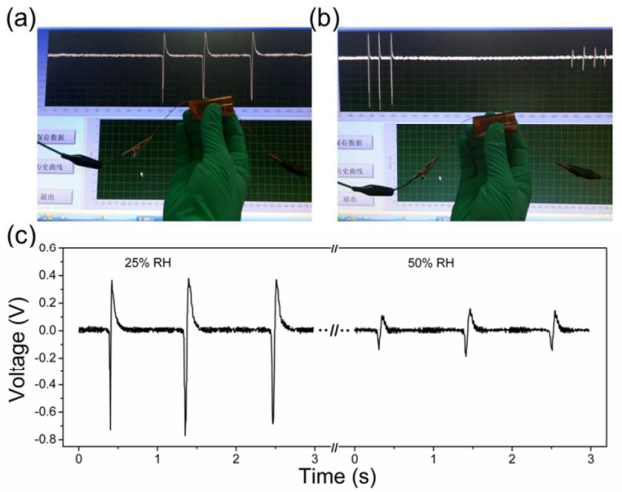

Fig. 7 The flexible self-powered humidity sensor can be driven by human finger movement. (a, b) A photograph of the flexible device driven by human finger at 25% and 50% RH, respectively. (b) The piezoelectric output of the device driven by human finger at 25% and 50% RH.

As shown in Fig. 7, the flexible device structure of the Co-doped ZnO NWs self-powered humidity sensor can convert tiny mechanical energy of human motion into an electrical signal. Fig. 7a and b show that the device is very flexible and can be easily deformed by human finger. The piezoelectric output of the device driven by human finger at 25% and 50% RH is shown in Fig. 7c, and the piezoelectric voltage is about 0.380 and 0.141 V, respectively. This result demonstrates the feasible applications of Co-doped ZnO NWs self-powered humidity sensor in our living environment. It should also be pointed that future work needs to be done on designing suitable device structures that can apply constant deformation for their practical applications.

Conclusions

In summary, high sensitive and repeatable self-powered humidity sensor has been realized from Co-doped ZnO NWs. The response of the Co-doped ZnO NG was as high as 454.2 upon exposure to 70% RH, much higher than that of undoped ZnO NWs (120.6). Such a high performance can be attributed to the piezo-surface coupling effect of the nanocomposites and more active sites introduced by the Co dopants. Our study demonstrated that introducing element dopant into the self-powered humidity sensor is a very effective way to enhance their piezo-humidity sensing performance

Acknowledgements

This work was supported by the National Natural Science Foundation of China (51102041 and 11104025), the Fundamental Research Funds for the Central Universities (N120205001 and N140505004), and the Program for New Century Excellent Talents in University (NCET-13-0112).

Notes and references

1 A. Tetelin, C. Pellet, C. Laville and G. N'Kaoua, *Sensor. Actuat. B-Chem.*, 2003, **91**, 211-218.
2 D. Bridgeman, J. Corral, A. Quach, X. J. Xian and E. Forzani, *Langmuir*, 2014, **30**, 10785-10791.
3 U. Mogera, A. A. Sagade, S. J. George and G. U. Kulkarni, *Sci. Rep.-Uk*, 2014, **4**, 10.1038/srep04103.
4 Y. H. Zhu, H. Li, J. Q. Xu, H. Yuan, J. J. Wang and X. X. Li, *CrystEngComm*, 2011, **13**, 402-405.
5 C. P. Zhao, X. W. Zhang, Y. P. Zhang, Y. L. Xing, X. J. Zhang, X. H. Zhang and J. S. Jie, *CrystEngComm*, 2012, **14**, 819-823.
6 L. L. Xing, C. H. Ma, Z. H. Chen, Y. J. Chen and X.-Y. Xue, *Nanotechnology*, 2011, **22**, DOI: 10.1088/0957-4484/22/21/215501.
7 Y. Yu, J. P. Ma and Y. B. Dong, *CrystEngComm*, 2012, **14**, 7157-7160.
8 K. P. Kadlag, P. Patil, M. J. Rao, S. Datta and A. Nag, *CrystEngComm*, 2014, **16**, 3605-3612.
9 W. Q. Fan, H. Y. Bai and W. D. Shi, *CrystEngComm*, 2014, **16**, 3059-3067.
10 J. L. Hou, C. H. Wu and T. J. Hsueh, *Sensor. Actuat. B-Chem.*, 2014, **197**, 137-141.
11 B. Yin, Y. Qiu, H. Q. Zhang, J. Y. Ji and L. Z. Hu, *CrystEngComm*, 2014, **16**, 6831-6835.
12 Y. M. Juan, S. J. Chang, H. T. Hsueh, T. C. Chen, S. W. Huang, Y. H. Lee, T. J. Hsueh and C. L. Wu, *Sensor. Actuat. B-Chem.*, 2015, **219**, 43-49.
13 Z. L. Wang, *Adv. Mater.*, 2012, **24**, 280-285.
14 F. R. Fan, L. Lin, G. Zhu, W. Wu, R. Zhang and Z. L. Wang, *Nano Lett.*, 2012, **12**, 3109-3114.
15 Y. B. Zheng, L. Cheng, M. M. Yuan, Z. Wang, L. Zhang, Y. Qin and T. Jing, *Nanoscale*, 2014, **6**, 7842-7846.
16 R. M. Yu, C. F. Pan, J. Chen, G. Zhu and Z. L. Wang, *Adv. Funct. Mater.*, 2013, **23**, 5868-5874.
17 X. Y. Xue, Y. X. Nie, B. He, L. L. Xing, Y. Zhang and Z. L. Wang, *Nanotechnology*, 2013, **24**, DOI: 10.1088/0957-4484/24/22/225501.
18 G. X. Zhu, H. Xu, Y. J. Liu, X. Xu, Z. Y. Ji, X. P. Shen and Z. Xu, *Sensor. Actuat. B-Chem.*, 2012, **166-167**, 36-43.
19 Y. J. Li, K. M. Li, C. Y. Wang, C. I. Kuo and L. J. Chen, *Sensor. Actuat. B-Chem.*, 2012, **161**, 734-739.
20 Y. Lin, Y. Wang, W. Wei, L. H. Zhu, S. P. Wen and S. P. Ruan, *Ceram. Int.*, 2015, **41**, 7329-7336.
21 X. B. Wang, Y. Yan, B. Hao and G. Chen, Dalton T., 2014, **43**, 14054-14060.
22 Y. M. Liu, Q. Q. Fang, M. Z. Wu, Y. Li, Q. R. Lv, J. Zhou and B. M. Wang, *J. Phys. D: Appl. Phys.*, 2007, **40**, 4592-4596.
23 M. Lee, J. Bae, J. Lee, C. S. Lee, S. Hong and Z. L. Wang, *Energy Environ. Sci.*, 2011, **4**, 3359-3363.
24 C. Q. Zhang, Z. B. Huang, X. M. Liao, G. F. Yin and J. W. Gu, *J. Coat. Technol. Res.*, 2012, **9**, 621-628.
25 E. Comini, G. Faglia, G. Sberveglieri, Z. W. Pan and Z. L. Wang, *Appl. Phys. Lett.*, 2002, 81, 1869-1871.

26 A. Erol, S. Okur, B. Comba, Ö. Mermer and M. Ç. Arıkan, *Sensor. Actuat. B-Chem.*, 2010, **145**, 174-180.
27 L. P. Chen and J. Zhang, *Sensor. Actuat. A-Phys.*, 2012, **178**, 88-93.
28 S. Jagtap and K. R. Priolkar, *Sensor. Actuat. B-Chem.*, 2013, **183**, 411-418.
29 D. Zhu, Y. M. Fu, W. L. Zang, Y. Y. Zhao, L. L. Xing and X. Y. Xue, *Sensor. Actuat. B-Chem.*, 2014, **205**, 12-19.
30 Y. X. Zhu, Q. F. Li, P. L. Wang, W. L. Zang, L. L. Xing and X. Y. Xue, *Mater. Lett.*, 2015, **154**, 77-80.
31 D. Zhu, T. X. Hu, Y. Y. Zhao, W. L. Zang, L. L. Xing and X. Y. Xue, *Sensor. Actuat. B-Chem.*, 2015, **213**, 382-389.
32 Y. M. Fu, Y. X. Nie, Y. Y. Zhao, P. L. Wang, L. L. Xing, Y. Zhang and X. Y. Xue, *ACS appl. Materi. Inter.*, 2015, **7**, 10482-10490.
33 Y. F. Hu, L. Lin, Y. Zhang and Z. L. Wang, *Adv. Mater.*, 2012, **24**, 110-114.
34 J. He and C. M. Lilley, *Nano Lett.*, 2008, **8**, 1798-1802.
35 Y. J. Lin, P. Deng, Y. X. Nie, Y. F. Hu, L. L. Xing, Y. Zhang and X. Y. Xue, *Nanoscale*, 2014, **6**, 4604-4610.
36 Y. M. Fu, W. L. Zang, P. L. Wang, L. L. Xing, X. Y. Xue and Y. Zhang, *Nano Energy*, 2014, **8**, 34-43.
37 L. Liu, S. C. Li, J. Zhuang, L. Y. Wang, J. B. Zhang, H. Y. Li, Z. Liu, Y. Han, X. X. Jiang and P. Zhang, *Sensor. Actuat. B-Chem.*, 2011, **155**, 782-788.
38 J. R. Huang, L. Y. Wang, C. P. Gu, M. H. Zhai and J. H. Liu, *CrystEngComm*, 2013, **15**, 7515-7521.
39 M. L. Yin and S. Z. Liu, *Mater. Chem. Phys.*, 2015, **149-150**, 344-349.
40 S. Kuriakose, B. Satpati and S. Mohapatra, *Phys. Chem. Chem. Phys.*, **16**, 12741-12749.
41 Y. Liu, Y. Jiao, Z. L. Zhang, F. Y. Qu, A. Umar and X. Wu, *ACS appl. Materi. Inter.*, 2014, **6**, 2174-2184.
42 C. H. Zhao, G. Z. Zhang, W. H. Han, J. C. Fu, Y. M. He, Z. X. Zhang and E. Q. Xie, *CrystEngComm*, 2013, **15**, 6491-6497.
43 P. Pattananuwat, M. Tagaya and T. Kobayashi, *Sensor. Actuat. B-Chem.*, 2015, **209**, 186-193.
44 J. D. Li, T. Fu, Y. J. Chen, B. K. Guan, M. Zhuo, T. Yang, Z. Xu, Q. H. Li and M. Zhang, *CrystEngComm*, 2014, **16**, 2977-2983.
45 H. Li, B. Liu, D. P. Cai, Y. R. Wang, Y. Liu, L. Mei, L. L. Wang, D. D. Wang, Q. H. Li and T. H. Wang, *J. Mater. Chem. A*, 2014, **2**, 6854-6862.

TOC

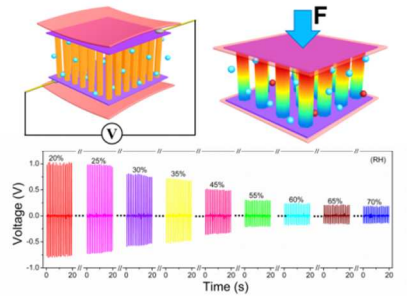

TOC text

Self-powered humidity sensor with high sensitivity and repeatability has been fabricated from Co-doped ZnO NW arrays. Such a high performance can be attributed to the piezo-surface coupling effect of the nanocomposites and more active sites introduced by the Co dopants.